Acta Chemica Scandinavica A 35 (1981) 559–567

Anionic and Cationic Species Formed in Irradiated $NaND_4$-tartrate Studied by ESR Spectroscopy and Pulse Radiolysis. Structure and Decay Mechanism Study

PER-OLOF SAMSKOG

The Studsvik Science Research Laboratory, S-611 82 Nyköping, Sweden

ESR spectroscopy and nanosecond pulse radiolysis have been used to study the species formed in single crystals of $NaND_4$-tartrate on irradiation. The primary reduction product $^-OOCCHODCHODCO\text{-}OD^-$ has an optical absorption maximum at 400 nm. It decays at +21 °C with a half life of 2.2 μs to $^-OOCCHODĊHCOO^-$. The activation energy for the anionic decay is 8.3 kcal mol^{-1}. The primary oxidation product $[^-OOCCHODCHODCOO^-]^+$ decays by decarboxylation to $^-OOCCHODĊHOD$. On further heating all secondary radicals are transformed to $^-OOCCHODĊODCOO^-$, which is stable at room temperature.

Primary reaction products formed by irradiation of single crystals of carboxylic acids and their salts have previously been investigated by ESR and ENDOR spectroscopy.[1] Both the reduction $R-ĊOOH^-$ and the oxidation $R-COȮ$ products have their unpaired electron localized on the carboxylic group. Neither of these primary products persist on warming the crystals to room temperature.

The experimental techniques used in this investigation are ESR spectroscopy and nanosecond pulse radiolysis. The structure, the decay kinetics and the optical absorption spectra for the radical anion $R-ĊOOH^-$ have been investigated in NaK-tartrate [2,3] (Rochelle salt), diK-tartrate [4] and in the present study in $NaNH_4$-tartrate. In diK-tartrate a new kind of cationic species was observed. The same observation has now been made in $NaNH_4$-tartrate. A proposal of the structure of such a cationic species is given.

EXPERIMENTAL

$NaNH_4$-tartrate ($NaNH_4C_4H_4O_6 \cdot 4H_2O$) was prepared by mixing equimolar amounts of Na_2-tartrate and $(NH_4)_2$-tartrate. Single crystals were grown from saturated aqueous solutions by slow evaporation at room temperature and were checked by polarized light. The deuterated crystals ($NaND_4C_4H_2D_2O_6 \cdot 4D_2O$) were obtained by several recrystallizations of the salt from heavy water. $NaNH_4$-tartrate crystals are orthorhombic and isomorphous to NaK-tartrate.[5] This means that there are four molecules in the unit cell. The crystal structure is not known. The morphology and reference axis system are shown in Fig. 1.

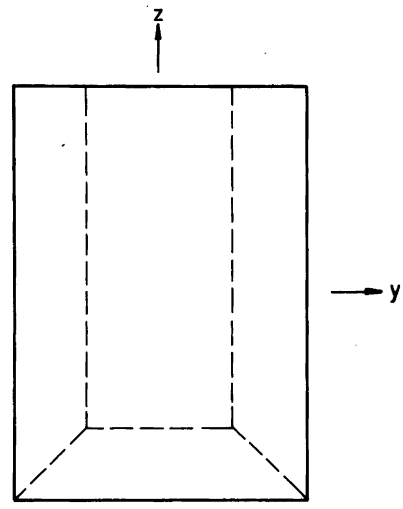

Fig. 1. Crystal morphology and the coordinate system used for $NaND_4$-tartrate.

0302-4377/81/080559-09$02.50

The crystals are elongated along the z-axis and the x, y, z axes were taken as the Cartesian co-ordinates.

In the pulse radiolysis experiments the crystals were placed in a cryostat and irradiated from opposite sides by single 3 ns pulses of 800 keV electrons from a double beam Febetron 708. Light from a pulsed 450 W Xenon lamp was used for analyzing the transient absorption and passed the sample at right angles to the electron beams. A photomultiplier tube recorded the light intensity and the transient signal was fed directly into a 100 MHz storage oscilloscope. The overall risetime of the system is about 5 ns. The optical path length was about 10 mm and the thickness of the crystals in the direction of the electron beams was 2 mm, which gives a fairly homogeneous dose distribution in the sample. Since the dose rate was very high, calorimetry was the most reliable method for dose measurement. The average dose measured was 142 krad/pulse. Calorimetry was also used for the relative dosimetry. For a more detailed description of the pulse radiolysis experimental setup see Ref. 2.

The crystals used for the ESR measurements were irradiated with a dose rate of 210 krad/h during 4 h in a ^{60}Co gamma cell at 77 K. The ESR spectra were then recorded as first derivatives with the aid of a Varian E9 spectrometer and both X and Q band were used. A flow of nitrogen gas was used in all experiments to thermostat the samples. The crystals were rotated about the x, y, z axes and the spectra were recorded for every 10° with the magnetic field perpendicular to the rotation axes. There is site splitting in the xy- and xz-planes but almost none in the yz-plane. Q band measurements were made in the same way at 90 K by rotation about the z-axis.

The G-value for CO_2 was found to be 3.4 measured on a Toepler pump. The crystals in the ampoule were irradiated at 77 K and then heated to 100 °C. The gas which evolved was measured after passing a cold trap, kept at −60 °C.

RESULTS AND ANALYSIS

Pulse radiolysis. The optical absorption spectrum of the transient species observed in $NaNH_4$-tartrate at room temperature is shown in Fig. 2. The absorption maximum is positioned at 400 nm. The same spectrum is measured for both the protonated and deuterated salts. The optical absorption decays with first order kinetics and has a half life of 2.2 μs at 21 °C. Since the decay is independent of the wavelength a single species is probably responsible for the optical absorption. The Arrhenius plot in Fig. 3 gives an activation energy of 8.3 kcal mol^{-1} (34.7 kJ mol^{-1}) for the decay of the species in both

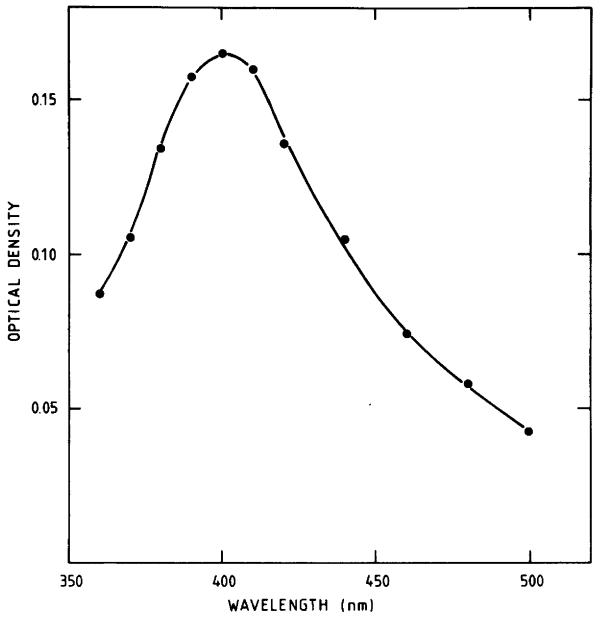

Fig. 2. Absorption spectrum of the transient species in irradiated $NaNH_4$-tartrate at 22 °C.

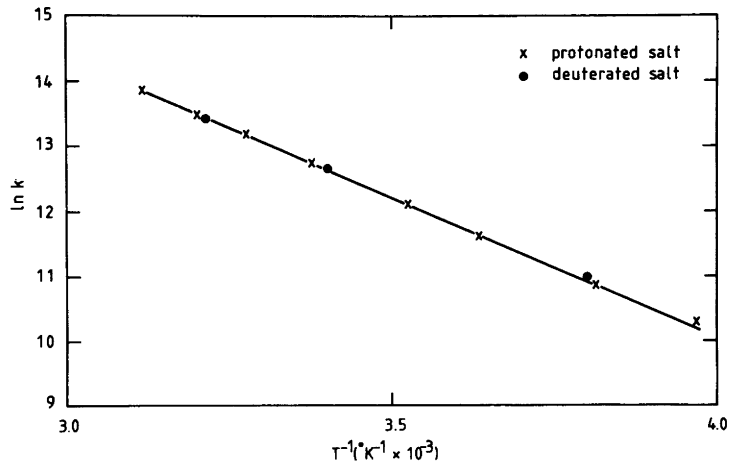

Fig. 3. Arrhenius plot for the decay of the radical anion ($\lambda_{max}=400$ nm) in irradiated $NaNH_4$-tartrate (protonated and deuterated salts).

the protonated and deuterated salts. From the optical densities, which refer to the end of the electron pulse, εG was calculated at 400 nm to be 520 ± 50 M^{-1} cm^{-1} $(100\ eV)^{-1}$, where ε is the molar extinction coefficient and G is the yield of molecules per 100 eV absorbed energy.

ESR spectroscopy. 77 K. Figs. 4a and 5a show spectra of $NaND_4$-tartrate irradiated and measured at 77 K. The protonated sample at this temperature gives in most directions rather broad and structureless spectra. This is probably due to appreciable hyperfine interactions from exchangeable protons. There are at least three different radicals present at 77 K. The ESR data for these radicals are collected in Table 1. Radical I has a resonance composed

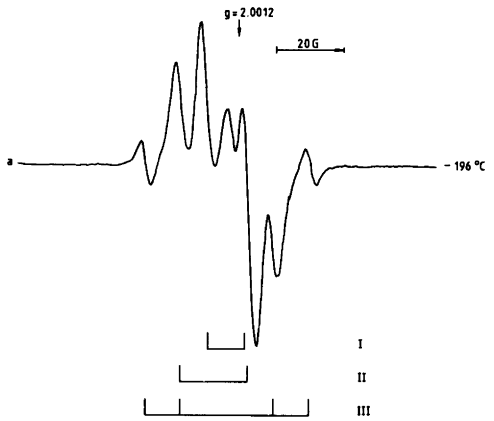

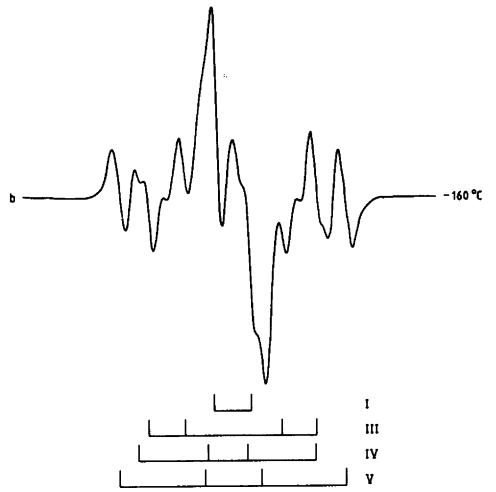

Fig. 4. ESR spectra of $NaND_4$-tartrate irradiated and measured at -196 °C after warming to different temperatures. The magnetic field is parallel to the z axis defined in the text.

of two lines, which probably are due to a hyperfine coupling to an H_β-hydrogen atom. No g-values are given for this radical because of overlapping hyperfine lines in many orientations. Nevertheless it is obvious that the g-value is rather isotropic ranging from 2.002 to 2.004. Radical I is interpreted as the radical anion (I). The same kind of radical anion has been observed in other tartrates.[2-4] In Rochelle

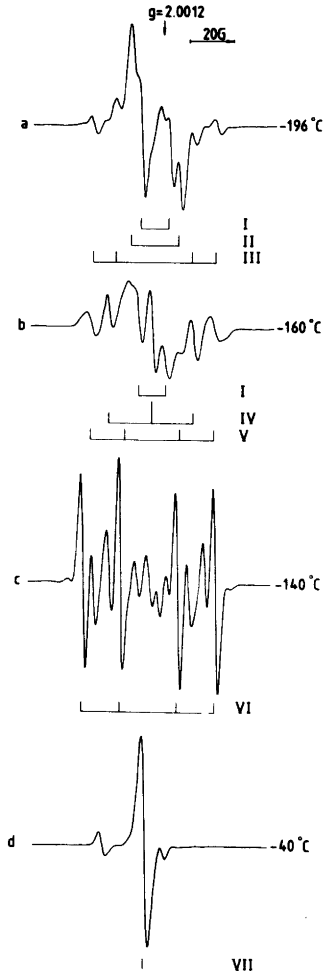

Fig. 5. ESR spectra of $NaND_4$-tartrate irradiated and measured at -196 °C after warming to different temperatures. The magnetic field is parallel to the x axis defined in the text. The gain is decreased with a factor 1.6 in b and a factor 4 in d.

salt [2,3] there was a coupling to the alkali ion Na^+. A similar coupling is not observed in $NaND_4$-tartrate.

$$^{-}OOC-CHOD-CHOD-\dot{C}\begin{matrix}-OD\\ O-\end{matrix} \qquad (I)$$

The second radical, denoted II, at 77 K has also a resonance composed of two lines. The isotropic hyperfine coupling suggests interaction between the unpaired electron and a β-hydrogen atom. These lines move towards the low magnetic field side at certain orientations, Fig. 4a. This anisotropy is caused by the shift in the g-values, which is confirmed by Q-band measurements, where the anisotropy due to the g-values becomes more pronounced.

Radical II was found to have g-values ranging from 2.002 to 2.006. A similar radical species was observed in diK-tartrate.[4] Radical II decays by a decarboxylation process (see below -160 °C). This process is typical for a radical cation of the RCOO type,[1] which is a σ radical. The unpaired electron occupies an antibonding molecular orbital which is a linear combination of oxygen 2p orbitals.[6] This radical cation is characterized by a very anisotropic g-value (*ca.* $2.02-2.002$). This is not, however, fulfilled by radical II in $NaND_4$-tartrate. There are two facts that indicate that radical II is some kind of cationic species, the decarboxylation process and the high yield of CO_2($G=3.4$).

The assignment of radical II is tentative. One possibility suggested by Professor M.C.R. Symons, is that there is a weak bonding between one of the OH groups and the $-CO_2\cdot$ group formed by electron loss, as indicated in (II).

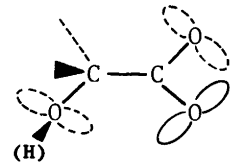

(II)

Such a stabilizing interaction would reduce the overall g-shift and the results for species II could well be explained by this species. Since the hyperfine coupling due to the β-hydrogen atom is rather large (Table 1), there must be a considerable spin density on the OH group.

The third radical observed at 77 K in Figs. 4a and 5a is denoted as III. The resonance is composed of four lines. The hyperfine couplings are isotropic indicating that there are two interacting β-protons. The data are listed in Table 1. The protonated salt gives additional hyperfine coupling with a maximum value of 5G due to an exchangeable proton. The radical III is identified as (III).

$$^{-}OOC-\dot{C}OD-\begin{matrix}H\\ |\\ C\\ |\\ OD\end{matrix}-H \qquad (III)$$

Table 1. Principal hyperfine coupling (G) and principal g-values for the different radicals in $NaND_4$-tartrate observed at 77 K.

Radical	Principal g	a_β
I $^-OOC-CHOD-CHOD-\dot{C}OOD^-$	– – –	10–13
II $[^-OOC-CHOD-CHOD-COO^-]^+$	2.0060 2.0033 2.0023	19–22
III $^-OOC-\dot{C}OD-CH_2OD$	2.0041 2.0034 2.0024	9–12 and 40–44

–160 °C. On thermal annealing of the sample to –160 °C radical II disappears and the resonances of radical IV and V appear, Fig. 5b. Data for these new radicals are collected in Table 2. Stick plots for these radicals are shown in Figs. 4b and 5b. The line positions for radical IV and V in the *yz*-plane are plotted in Fig. 6. The plot shows that both radicals have an anisotropic hyperfine interaction and a nearly isotropic g-factor. The hyperfine interaction is due to one α- and one β-proton coupling. The observed extra hyperfine coupling for both radicals of approximately 5 G in the protonated salt indicates that an OH group is close to the unpaired electron. The coupling constants and deuteration effects suggest the radicals to be (IV and V), with different conformation for the β-proton.

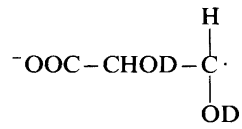

(IV and V)

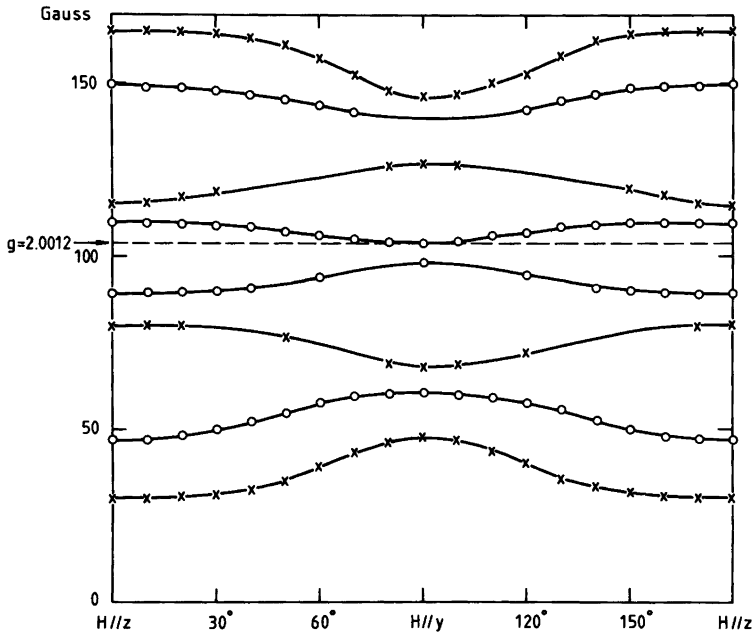

Fig. 6. The positions of the different lines of radical IV and V plotted for different crystal orientations in the *yz*-plane at –160 °C. The circles represent radical IV and the crosses represent radical V.

Table 2. Principal hyperfine couplings (G) and principal g-values for different radicals in $NaND_4$-tartrate observed after annealing the sample.

Radical	Principal values g	a_α	a_β
IV	2.0035	31	
$^-OOC-CHOD-\dot{C}HOD$	2.0024	2	18–21
	2.0021	13	
V	2.0037	27	
$^-OOC-CHOD-\dot{C}HOD$	2.0030	16	39–42
	2.0024	9	
VI	2.0029	31	
$^-OOC-CHOD-\dot{C}H-COO^-$	2.0026	20	43–47
	2.0020	10	
VII	2.0046	–	
$^-OOC-CHOD-\dot{C}OD-COO^-$	2.0035	–	0–5
	2.0021	–	

–140 °C. The primary radical I disappears at –140 °C and at the same rate a new radical VI appears, as shown in Fig. 5c. Once again a four line spectrum is obtained. The angular variation of the line positions in the *yz*-plane is plotted in Fig. 7, which shows the typical variation for a radical consisting of one α- and one β-hydrogen atom. The data for the g-values, α-H and β-H coupling constants are collected in Table 2. The protonated salt gives no superhyperfine structures from exchangeable protons. Similar observations were made in NaK [2,3] and diK-tartrate [4] and the radical responsible for the observed spectrum is most likely (VI).

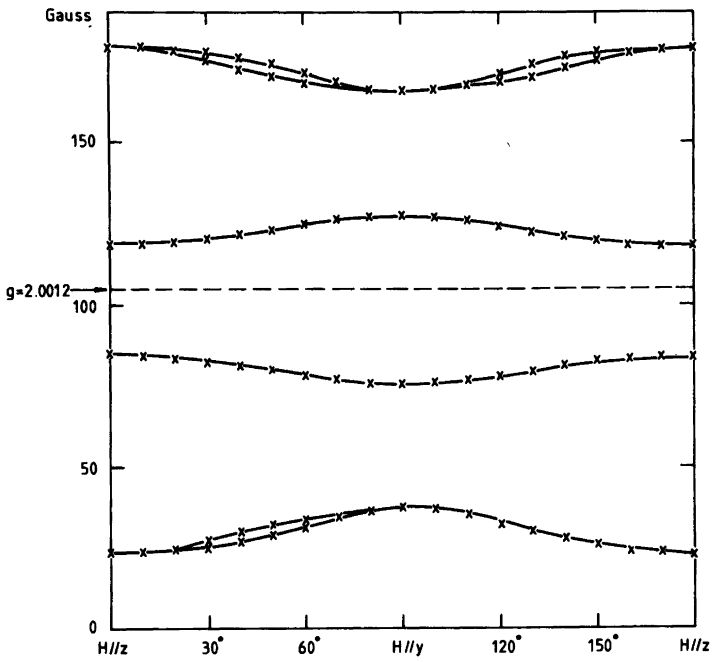

Fig. 7. The line positions of radical VI for different crystal orientations in the *yz*-plane at –140 °C.

Table 3. Optical absorption maximum (λ_{max}), activation energy (E_a), pre-exponential factor (A) and εG for radical anions in different compounds.

Compound	Radical	λ_{max} nm	E_a kcal/mol	A $s^{-1}\,M^{-1}\,cm^{-1}$	εG $(100\,eV)^{-1}$	Ref.
$NaNH_4$-tartrate	$R-C-\dot{C}OOH^-$	400	8.3	4.6×10^{11}	520	This work
NaK-tartrate	$R-C-\dot{C}OOH^-$	405	7.5	4.4×10^{12}	2560	2,3
K_2-tartrate	$R-C-\dot{C}OOH^-$	455	9.4	8.9×10^{13}	3000	4
Glycine-d_3	$D_3^+NCH_2\dot{C}OOD^-$	480	5.5	8.9×10^{9}	850	10a
Alanine-d_3	$D_3^+NCH(CH_3)\dot{C}OOD^-$	415	10.9	1.3×10^{14}	985	10b
α-Amino isobutyric acid	$D_3^+NC(CH_3)_2\dot{C}OOD^-$	365	11.7	1.9×10^{13}	–	10b
Chloroacetic acid	$ClCH_2\dot{C}OOH^-$	395	13.9	2.0×10^{16}	1800	10c
Bromoacetic acid	$BrCH_2\dot{C}OOH^-$	440	12.3	1.1×10^{16}	–	10d

(VI)

−40 °C. At about −40 °C the resonances of radicals IV, V and VI decay at approximately the same time. A new resonance VII appears at the same rate, Fig. 5d. This resonance is a single line in most orientations except when the magnetic field is parallel or nearly parallel to the z-axis. In that direction the single line is split into a doublet with a maximum coupling of 5 G. This small hyperfine coupling is due to a β-hydrogen atom. Data for species VII are listed in Table 2. Radical VII still persists after annealing the sample to room temperature. The protonated sample has an additional coupling due to an exchangeable proton. This radical is identified as (VII). It could not be ascertained whether radical III also ends up in the room temperature stable radical VII.

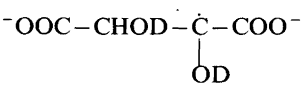

(VII)

DISCUSSION

The primary reduction product and its reaction. The primary reduction products in carboxylic acids and their salts have their unpaired electrons almost entirely on the carboxylic carbons.[1,3] It seems as though the anions in carboxylic acids are in their protonated form. The reaction mechanism for the decay of the radical anion in $NaND_4$-tertrate is the same as in NaK-[2,3] and diK-tartrate.[4]

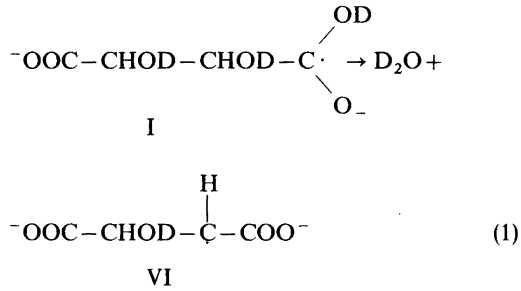

(1)

In other carboxylic acids than tartrates this β-elimination reaction has not been observed. Instead the primary reduction product decays to $R\dot{C}{=}O$ by elimination of OH^- from the carboxylic group.[7-9] It seems as if reaction (1) is typical for hydroxy acids and their salts.

Optical absorption of radical anions. From the pulse radiolysis measurements a half life for the optical transients of 1 min at −140 °C was calculated by extrapolation of the Arrhenius plot, Fig. 3. This is in good agreement with the observed decay of radical I, Fig. 5b, and the growth of radical VI, Fig. 5c. Therefore the 400 nm optical absorption is assigned to the radical anion. Reaction (1) has an activation energy of 8.3 kcal mol^{-1}.

In Table 3 are listed optical properties for radical anions in different compounds. All data are obtained from single crystal studies. By comparing the kinetics of the transient optical absorptions with the decay of the line intensities in the ESR spectra it has been possible to assign the optical transients to the radical anions for the tabulated compounds, which all contain a carboxylic group. All anions are stabilized in their protonated form and they decay by a β-elimination reaction. It is noticeable that all optical maxima lie in the visible region.

The activation energies for the decay of the radical anions are almost equal within the same type of reaction, dehydration, deamination and dehalogenation, except for glycine-d_3. The discrepancies in the values of the pre-exponential factors are difficult to explain. The extremely low value of εG for $NaNH_4$-tartrate is probably caused by a lower yield of radical anions in this salt compared to the other two tartrates. This conclusion is confirmed by comparing the radical yield from the ESR spectrum of the different salts.

The primary oxidation product and its reaction. The primary oxidation product, radical II, decays at −160 °C, Figs. 4 and 5. The secondary radicals are both of the form $^{-}OOC-CHOD-\dot{C}HOD$, which can be formed by decarboxylation of the primary oxidation product. An accepted pathway for the decomposition of the radical cation is (2);[1]

$$(^{-}OOC-\underset{\text{II}}{CHOD}-CHOD-COO^{-})^{+} \rightarrow {}^{-}OOC-\underset{\text{IV, V}}{CHOD}-\dot{C}HOD+CO_2 \qquad (2)$$

CO_2 is formed with a *G*-value of 3.4. It is noticeable that two different types of decarboxylation products are formed. This can be explained if a primary oxidation product is formed in both carboxylic groups. No clear evidence for the formation of two types of primary oxidation products at 77 K has been obtained.

Secondary products and their reactions. Radical III, which is already present at 77 K is a secondary product. This is probably formed from a radical cation through decarboxylation, followed by a intramolecular hydrogen transfer (3).

$$^{-}OOC-CHOD-\dot{C}HOD \rightarrow {}^{-}OOC-\underset{\text{III}}{\dot{C}OD}-CH_2OD \qquad (3)$$

A similar reaction is not observed for radicals IV and V. The precursor of radical III might exist in an excited state. This could be the reason why reaction (3) occurs below 77 K.

A similar reaction was proposed to occur in disodium succinate[11] and diK-tartrate.[4] The assumption of the precursor of radical III leads to the conclusion that two different types of radical cations are formed originally. The first type is very reactive and has already decomposed at 77 K. The second type is more stable because of the interaction between one OH-group and the $-CO_2\cdot$ group(II).

Fig. 5d shows that the terminus for all radicals is the radical VII, which is stable at room temperature. This transformation occurs at about −40 °C for both the secondary oxidation products (4) and the secondary reduction product (5).

$$^{-}OOC-CHOD-\underset{\text{IV}}{\dot{C}HOD}+{}^{-}OOC-\underset{\text{V}}{CHOD}-CHOD-COO^{-} \rightarrow \qquad (4)$$

$$\rightarrow {}^{-}OOC-CHOD-\underset{\text{VII}}{\dot{C}OD}-COO^{-}+{}^{-}OOC-CHOD-CH_2OD$$

$$^{-}OOC-CHOD-\underset{\text{VI}}{\dot{C}H}-COO^{-}+{}^{-}OOC-CHOD-CHOD-COO^{-} \rightarrow \qquad (5)$$

$$\rightarrow {}^{-}OOC-CHOD-\underset{\text{VII}}{\dot{C}OD}-COO^{-}+{}^{-}OOC-CHOD-CH_2-COO^{-}$$

This kind of intermolecular reactions has been proposed to occur in *dl*-tartaric acid[12] and disodium succinate.[11]

The radical III is not stable at room temperature. It is probably transformed to product VII. Because of serious overlap by other hyperfine lines it is difficult to observe at what temperature this transformation occurs. The reaction (6) is analogous to reactions (4) and (5).

$$^{-}OOC-\underset{\text{III}}{\dot{C}OD}-CH_2OD+{}^{-}OOC-CHOD-CHOD-COO^{-} \rightarrow \qquad (6)$$

$$\rightarrow {}^{-}OOC-CHOD-\underset{\text{VII}}{\dot{C}OD}-COO^{-}+{}^{-}OOC-CHOD-CH_2OD$$

REFERENCES

1. Box, H. C. *Radiation Effects, ESR and ENDOR Analysis*, Academic, New York 1977, Chapters 6 and 7.
2. Samskog, P. O., Nilsson, G. and Lund, A. *J. Chem. Phys. 68* (1978) 4986.

3. Samskog, P. O., Lund, A., Nilsson, G. and Symons, M. C. R. *Chem. Phys. Lett. 66* (1979) 199.
4. Samskog, P. O., Lund, A., Nilsson, G. and Symons, M. C. R. *Radiat. Phys. Chem. 16* (1980) 359.
5. Jona, F. and Shirane, G. *Ferroelectric Crystals*, International Series of Monographs on Solid State Physics, Pergamon, New York 1962, p. 303.
6. Iwasaki, M., Minakata, K. and Toriyama, K. *J. Am. Chem. Soc. 94* (1971) 3533.
7. McCalley, R. C. and Kwiram, A. L. *J. Am. Chem. Soc. 92* (1970) 1441.
8. McCalley, R. C. and Kwiram, A. L. *J. Chem. Phys. 53* (1970) 2541.
9. Yim, M. B. and Klinck, R. E. *J. Chem. Phys. 60* (1974) 538.
10. a. Samskog, P. O., Gillbro, T. and Nilsson, G. *Chem. Phys. Lett. 64* (1979) 162; b. Samskog, P. O., Nilsson, G., Lund, A. and Gillbro, T. *J. Phys. Chem. 84* (1980) 363; c. Samskog, P. O., Lund, A., Nilsson, G. and Symons, M. C. R. *Chem. Phys. 42* (1979) 363; d. Lund, A., Samskog, P. O. and Nilsson, G. *Chem. Phys. 57* (1981) 399.
11. Bales, B. L., Schwartz, R. N. and Hanna, M. W. *J. Chem. Phys. 51* (1969) 1974.
12. Moulton, G. C. and Cernansky, B. *J. Chem. Phys. 53* (1970) 3022.

Received January 16, 1981.